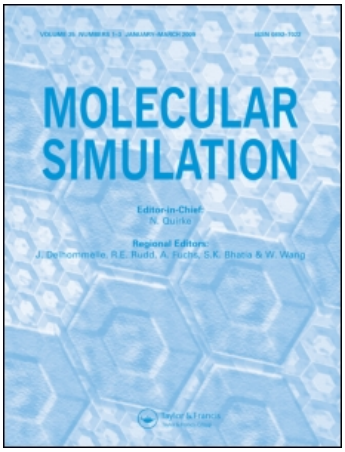

Molecular Simulation
Publication details, including instructions for authors and subscription information:
http://www.informaworld.com/smpp/title~content=t713644482

A new semi-empirical model for the oxidation of PAHs physisorbed on soot. I. Application to the reaction C_6H_6+OH

G. Hantal[ab]; S. Picaud[a]; B. Collignon[a]; P. N. M. Hoang[a]; M. T. Rayez[c]; J. C. Rayez[c]
[a] Institut UTINAM - UMR CNRS 6213, Université de Franche-Comté, Besançon Cedex, France [b] Laboratory of Interfaces and Nanosized Systems, Institute of Chemistry, Eötvös Loránd University, Budapest, Hungary [c] Institut des Sciences Moléculaires - UMR CNRS 5255, Université de Bordeaux I, Talence Cedex, France

To cite this Article Hantal, G. , Picaud, S. , Collignon, B. , Hoang, P. N. M. , Rayez, M. T. and Rayez, J. C.(2009) 'A new semi-empirical model for the oxidation of PAHs physisorbed on soot. I. Application to the reaction C_6H_6+OH', Molecular Simulation, 35: 12, 1130 — 1139
To link to this Article: DOI: 10.1080/08927020902874016
URL: http://dx.doi.org/10.1080/08927020902874016

Molecular Simulation
Vol. 35, Nos. 12–13, October–November 2009, 1130–1139

Taylor & Francis
Taylor & Francis Group

A new semi-empirical model for the oxidation of PAHs physisorbed on soot. I. Application to the reaction C_6H_6 + OH†

G. Hantal[ab], S. Picaud[a]*, B. Collignon[a], P.N.M. Hoang[a], M.T. Rayez[c] and J.C. Rayez[c]*

[a]*Institut UTINAM – UMR CNRS 6213, Université de Franche-Comté, F-25030 Besançon Cedex, France;* [b]*Laboratory of Interfaces and Nanosized Systems, Institute of Chemistry, Eötvös Loránd University, Pázmány Péter stny. 1/a, H-1117 Budapest, Hungary;* [c]*Institut des Sciences Moléculaires – UMR CNRS 5255, Université de Bordeaux I, F-33405 Talence Cedex, France*

(*Received 9 January 2009; final version received 5 March 2009*)

In the present paper, we have used a new semi-empirical method to characterise the oxidation by OH of a benzene molecule adsorbed on a soot surface modelled by a graphene-like cluster. This method is based on an electrostatic and induction contribution calculated at the self-consistent field AM1 level associated with a sum of two-body dispersion terms of the $C^{(6)}/R^6$ form. This so-called AM1-D method has been used to compare the characteristics of the oxidation reaction for the adsorbed benzene with those of the corresponding reaction in the gas phase. The main conclusion of the present work is a clear inhibition of the oxidation process by the adsorption of the benzene molecule on a well-defined graphene-like surface. This conclusion is in qualitative agreement with experimental observations, concerning larger PAH molecules.

Keywords: semi-empirical method; soot; PAH; oxidation

1. Introduction

Polycyclic aromatic hydrocarbons (PAHs) are chemical pollutants ubiquitous in the atmosphere, aerosols, soils and sediments. They are mainly formed as by-products of combustion processes under oxygen-deficient conditions, and many of them and their degradation products are known or suspected allergens and carcinogens [1].

It has been long understood that the reactive fate of volatile PAHs (less than 3–4 rings) is governed by gas-phase reactions with the hydroxyl (OH) radical. However, due to their low-vapour pressure and aromaticity, heavier PAHs are mostly adsorbed on fine carbonaceous particles [2], where they are subject of a wide range of heterogeneous chemical reactions which depend on the particle composition [3–7]. This heterogeneous reactivity may thus be more important than the corresponding gas-phase reactions as sink for these compounds. Moreover, heterogeneous reactions of particle-bound PAHs may change the microphysical properties of the particle by making it more hygroscopic and hence modifying its cloud nucleation properties [8]. These heterogeneous reactions can also influence the atmospheric residence times of the carbonaceous particles and consequently their direct and indirect effects on climate [9,10].

During the incomplete combustion of carbonaceous fuels, PAHs are formed concurrently with soot particles and they play a significant role in soot formation and subsequent particle growth [11]. Soot is ubiquitous in the environment, where it has been observed to comprise tens of percent of the total aerosol carbon in both rural and urban areas [12,13]. Because PAHs have a high affinity for carbonaceous materials, adsorption of PAHs on soot may be an important mechanism affecting the gas–particle partitioning of PAHs [14].

Despite the importance of PAHs and soot particles' interactions, their actual effect on the radiative and chemical budgets of the atmosphere is still poorly known and some of this uncertainty is due to the lack of knowledge about the physico-chemical properties of the soot substrate [15,16]. Fresh soot particles consist of spherical primary carbonaceous particles that aggregate into larger clusters of fractal-like shapes [17]. These primary particles are often made of nanocrystallites containing graphite-type layers arranged in an onion-like structure, with diameters ranging between 20 and 50 nm [18,19]. Soot particles are usually associated with organic and inorganic soluble materials at their surfaces. One of the major problems is thus that soot is not a well-defined chemical substance [20]. Therefore, model particles are often used as a first approach to study atmospheric chemical processes as they are simpler and better characterised than natural particles [21,22]. There are several types of soot used for laboratory studies of atmospheric effects: commercial soot [23], spark-discharge soot [24,25] and soot resulting from the combustion of hydrocarbon fuels in different burners [26,27]. However,

†This paper is dedicated to the memory of our friend Jose Antonio Mejias who initiated our work on soot surfaces.

*Corresponding authors. Emails: sylvain.picaud@univ-fcomte.fr; jc.rayez@ism.u-bordeaux1.fr

ISSN 0892-7022 print/ISSN 1029-0435 online

DOI: 10.1080/08927020902874016
http://www.informaworld.com

different types of soot differ in particle size, specific surface area, structure and composition, and thus they may differ in chemical properties. As a consequence, studies of the physico-chemistry of PAHs on soot surfaces are very scarce. Up to now, there is only a limited number of controlled laboratory [28,29] or field [30,31] studies on the adsorption of gas-phase PAHs onto soot, and, to our best knowledge, there is only one paper devoted to the experimental study of the uptake of aromatic hydrocarbons onto soot with a known surface area, as a function of temperature and partial pressure [4].

In a recent study, Esteve et al. [21] have characterised the role of OH, NO_2 and NO radicals on the reactivity of 11 polyaromatic compounds adsorbed on graphite particles chosen as a model of atmospheric carbonaceous particles. The results showed that the reaction of particulate–PAHs with NO is negligible under atmospheric conditions, whereas in the case of the NO_2 reaction, significant differences in the reactivities have been observed. Moreover, all PAHs present similar rate constants while reacting with OH, and, compared to the reactivity in the gas phase, the heterogeneous reaction with OH radicals seems to show a potential inhibiting effect of the graphite surface, meaning that the mechanisms may be sensibly different [21].

From a theoretical point of view, structural and energetic information on the interaction between PAHs and carbonaceous surfaces like soot is also very scarce, primarily due to the fact that these systems are too large for tractable *ab initio* calculations. Indeed, a theoretical realistic simulation of intermolecular forces requires high-level electronic quantum calculations to account for dispersion effects. The expression 'high level quantum calculations' means the use of very large basis sets and a precise description of the correlation energy. Even for a simple perturbative approach, double excitations on two interacting molecules are necessary to mimic (in general rather poorly) dispersion effects. Then, the most accurate methods for determining the geometry and binding energy of PAHs clusters are correlated quantum chemistry calculations that use very large correlation-consistent basis sets. Moreover, very large basis sets are necessary to minimise both the basis set convergence error and the basis set superposition error. Such high-level calculations require a great amount of computational resources [32] and if they are possible for, e.g. benzene dimers [33], they are not conceivable for larger systems.

Recently, an interesting method – the Hartree–Fock Dispersion model (HFD) – has been introduced by Gonzalez et al. [34,35] to calculate the structure and binding energy of aromatic clusters, following the work originally proposed by Hepburn et al. [36]. In this HFD method, the calculation of the intermolecular energies combines an *ab initio* self-consistent field (SCF) interaction energy with an empirical dispersion energy from the London theory, i.e. an analytical approach much more efficient to describe dispersion than the direct calculation from electronic correlation effects [34]. The accuracy of this method has been tested in computing the equilibrium geometries and the binding energies of the van der Waals dimers of benzene, naphthalene, anthracene and pyrene, as well as those of the naphthalene trimer [35]. However, even the HFD method is prohibited for a theoretical characterisation of the PAHs/soot interactions, when considering large size PAHs and/or large graphite clusters modelling the soot surface. We have thus introduced, in a recent paper [37], a new method where the SCF calculations are performed at a semi-empirical level by including explicitly the valence electrons only. This method, the so-called SE-D method, combines the semi-empirical description of the electrostatic and induction interactions to a sum of two-body London dispersion terms of the $C^{(6)}/R^6$ form. The empirical parameters of this method have been fitted on a set of *ab initio* and experimental results for 22 PAHs dimers and mixed complexes, aiming at defining a transferable interaction potential for the calculations of dispersion energy between aromatic molecules and large graphite clusters [37]. Three sets of transferable parameters have thus been determined for combination with electrostatic and induction interactions performed at the AM1, PM3 or MNDO level of theory, with, however, slightly better results when the dispersion parameters are combined with the AM1 and PM3 methods than with the MNDO method [37,38].

It is worth mentioning that such an approach that aims at describing intermolecular interactions in large carbonaceous systems on the basis of semi-empirical calculations shows similarities with methods recently developed to improve the semi-empirical description of other systems for which refined quantum calculations are too costly. For example, electrostatic and dispersion corrections have been brought to the AM1 or PM3 semi-empirical energy to reproduce correctly the long-range behaviour of the interaction potential in hydrogen bonded systems [39–41]. Similarly, an atom–atom pairwise additive dispersion potential has also been recently added to a semi-empirical description of the intermolecular interactions in biomolecules [42].

In the present paper, we make use of the SE-D method to characterise the oxidation mechanisms of PAH molecules adsorbed at the soot surface modelled by a large carbon cluster of the graphene type. Such a large cluster has been previously used to model soot surfaces interacting with water molecules using *ab initio* approaches [43–45]. The theoretical backgrounds of our study are given in Section 2, and, as a first application, the results of the detailed investigation of the heterogeneous oxidation reaction of benzene adsorbed on soot are then presented in Section 3. These results are compared with those obtained in the gas phase and they are discussed on the basis of experimental observations in Section 4.

2. Theoretical backgrounds

2.1 The SE-D method

In this section, we briefly recall the main basis of the SE-D model [37,38]. In this model, a dispersion term (U_d) is added to a semi-empirical determination of the electrostatic and induction interactions to account for dispersion forces in the calculation of the total energy. This total energy for a PAH adsorbed on a carbonaceous particle modelling a soot surface is thus written as

$$U_{\mathrm{SE-D}} = U_{\mathrm{SE}} + f \times U_{\mathrm{D}}, \tag{1}$$

where U_{SE} is the semi-empirical energy calculated at the AM1, PM3 or MNDO level of theory, U_{D} is the dispersion energy and f is a damping function used to avoid singularities in the dispersion term at short intermolecular distances. Note that these semi-empirical methods are proposed to reproduce, within an given average accuracy, geometries, heats of formation and some other thermodynamical data. These quantities are mainly due to 'chemical forces' which are responsible for bond energies, i.e. energy differences between separated fragments and the interacting systems at equilibrium distances. However, due to the reduced basis set used (valence atomic orbitals), it is impossible to reproduce a long-range quantum effect like dispersion. It is already almost impossible to do it with a 'reasonably good' *ab initio* approach. On the contrary, long-range electrostatic and induction effects, which are not quantum in nature but essentially classical (especially electrostatic effects), are included in a more or less realistic way in the calculations by the SCF procedure itself. The electrostatic interaction energy is given by the first SCF iteration and the induction energy at the SCF convergence since the electronic cloud, which corresponds to the average electronic field felt by each electron, reaches its final shape at the end of the SCF iterations. It turns out that the introduction of a sum of $-R^{-6}$ terms added at long distance to the SCF energy appears as an elegant way to include dispersion, even if it requires some 'savoir-faire' for the estimation of these terms.

The dispersion contribution to the total energy is thus expressed as [46]

$$f \times U_{\mathrm{D}} = -\sum_{i=1}^{N_g}\sum_{j=1}^{N_p} \frac{1}{(1+\mathrm{e}^{\alpha(R_0-R_{ij})})} \times \frac{\left[C_i^{(6)} C_j^{(6)}\right]^{1/2}}{R_{ij}^6}, \tag{2}$$

where N_g and N_p are the total number of atoms on the carbonaceous surface and in the PAH molecule considered, respectively. R_{ij} is the interatomic distance between a surface atom i and the jth atom of the PAH molecule, and $C^{(6)}$ represents the two-body dispersion coefficients used to calculate the C—C, C—H and H—H interactions. The damping function $f(R_{ij})$ has the two-parameter hyperbolic tangent function form proposed by Gonzales et al. [34,35], in which α and R_0 are two empirical parameters that monitor the behaviour of the damping function, and thus of the dispersion interaction, as a function of the interatomic distances R_{ij}.

The dispersion parameters α, R_0 and $C_j^{(6)}$ of the SE-D approach have been fitted for the combination with a semi-empirical calculation of the SCF contribution to the interaction energy. These parameters have been proved to be transferable from one PAH to another [37,38]. Here, we choose the SE-D set of parameters suitable for use with the semi-empirical AM1 method because it has proven to give slightly more reliable results than the set of parameters suitable for use with the PM3 and MNDO methods (see Ref. [37]). However, the present study is not limited to the calculation of the interaction between PAHs and soot surface because it aims also at characterising the oxidation of the adsorbed PAHs by the OH radical. We thus extend here the SE-D method to the calculations of the OH–PAH and OH–soot interactions, which are then written as

$$U_{\mathrm{AM1-D}}^{\mathrm{OH}} = U_{\mathrm{AM1}}^{\mathrm{OH}} - \sum_{i=1}^{N} \frac{1}{(1+\mathrm{e}^{\alpha^{\mathrm{OH}}(R_0^{\mathrm{OH}}-R_{\mathrm{iO}})})} \times \frac{\left[C_{\mathrm{O},i}^{(6)}\right]}{R_{i\mathrm{O}}^6}, \tag{3}$$

where the semi-empirical calculations are performed at the AM1 level for the consistency with the calculations of the PAH–soot interactions. The sum over i includes the total number N of carbon atoms in the system considered (soot + PAH), and the $C_{\mathrm{O},i}^{(6)}$ parameter for the oxygen–carbon interactions is taken from the literature [47]. Note that, all the hydrogen atoms are neglected in the calculations of the OH–soot and OH–PAH interactions. This assumption is based on the very weak contribution of these terms to the dispersion interactions in water–carbonaceous systems [48,49]. Determining the best values for the α^{OH} and R_0^{OH} parameters of the damping function is a delicate task which will be detailed below. All the parameters used in the present calculations are given in Table 1.

Table 1. Selected parameters for the dispersion contribution to the SE-D potential calculated with the semi-empirical AM1 method. The parameters $C_{\mathrm{C}}^{(6)}$, $C_{\mathrm{H}}^{(6)}$, and $C_{\mathrm{OC}}^{(6)}$ are given in kJ mol^{-1} Å^6.

	Benzene
$C_C^{(6)}$	2207.94
$C_{\mathrm{H}}^{(6)}$	48.6
$C_{\mathrm{OC}}^{(6)}$	1923.51
α	3.96
R_0	2.68
α^{OH}	64.00
R_0^{OH}	2.75

Note: α is given in Å^{-1} and R_0 in Å.

2.2 Energetics of the oxidation reaction

The mechanism of the oxidation reaction of PAH molecules by the OH radical is illustrated by the reaction scheme given in Figure 1.

In the first step of the reaction, a complex is formed between the reactants (the so-called pre-reactive complex, PRC) that, in the second step, transforms to the transition state (TS). Finally, the reaction results in the product that contains an sp^3 carbon atom and a π electron system with one missing electron. Defining the energies with respect to a reference state corresponding to the reactants far from each other, the PRC is located in an energy well (i.e. it corresponds to the negative energy E_1) while the TS corresponds to an energy barrier ($E_1 - E_2$) along the reaction path. Such a transition state formed with the OH radical was found both theoretically and experimentally in the case of hydrocarbons [50], and aromatic hydrocarbons such as benzene [51–53], toluene [54] and phenol [55].

2.3 Kinetics of the oxidation reaction

The kinetics of the oxidation mechanism presented in Figure 1 is governed by rate constants corresponding to the separate elementary reaction steps. The two first steps, schematised as

$$\mathrm{OH} + \mathrm{PAH} \underset{k_{-1}}{\overset{k_1}{\rightleftharpoons}} \mathrm{PRC}, \tag{4}$$

correspond to the formation of the PRC, characterised by the rate constant k_1, and to the decay of the PRC to the reactants, governed by the rate constant k_{-1}. Then, the formation of the product through the transition state is characterised by the rate constant k_2 as

$$\mathrm{PRC} \xrightarrow{k_2} \mathrm{Product}. \tag{5}$$

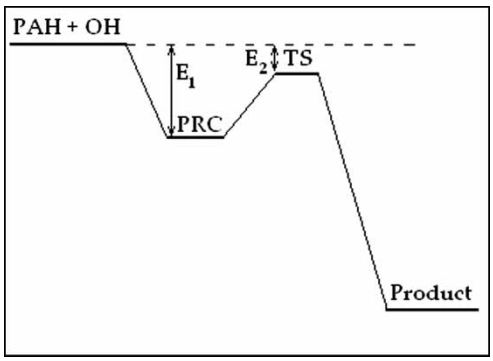

Figure 1. Schematic of the oxidation reaction of PAH molecules by OH radical. The energy of the reactants (PAH + OH) is taken as the reference state for the definition of the energies. PRC and TS define the pre-reactive complex and the transition state, respectively.

Finally, it should be taken into account that the PRC can be quenched by collisions with neutral particles as,

$$\mathrm{PRC} + \mathrm{M} \xrightarrow{k_3} \mathrm{PRC_{inactive}} + \mathrm{M}. \tag{6}$$

This quenching step is characterised by the second order rate constant k_3 and M can be any neutral particle that does not experience any chemical transformation during the collision.

Then, the global reaction rate for the oxidation process (i.e. the reaction rate for the formation of the product from the reactants) can be written in the following form:

$$r = \frac{\mathrm{d[Product]}}{\mathrm{d}t} = k_2[\mathrm{PRC}] = k[\mathrm{OH}][\mathrm{PAH}]. \tag{7}$$

If we assume now that the PRC is in a quasi-steady state, then we arrive at the following expression for the total rate constant

$$k = \frac{k_1 k_2}{k_{-1} + k_2 + k_3[\mathrm{M}]}. \tag{8}$$

We can now make two additional assumptions. First, we consider the existence of an equilibrium between the reactants and the PRC, such that the decay of the PRC to reactants is much faster than the formation of the product, i.e.

$$k_{-1} \gg k_2. \tag{9}$$

Moreover, under tropospheric conditions, the pressure is less enough so that the collisions with neutral particles are considerably rare events. We can thus assume that

$$k_2 \gg k_3[\mathrm{M}]. \tag{10}$$

Finally, for the total rate constant, we obtain

$$k = k_2 \frac{k_1}{k_{-1}} = k_2 K, \tag{11}$$

where K is the equilibrium constant of the formation of the PRC. Note that, we arrive at an expression similar to the one proposed by Atkinson and Cvetanovic [56] for the characterisation of the addition of O atoms to olefins.

2.4 Calculations of K *and* k_2

The canonical equilibrium constant K for a gas-phase process is given by

$$K = \frac{Q_{\mathrm{PRC}}}{Q_{\mathrm{PAH}} Q_{\mathrm{OH}}} \mathrm{e}^{-E_1/k_{\mathrm{B}}T}, \tag{12}$$

where E_1 is the energy of the PRC with respect to the reference state (PAH + OH at an infinite distance from each other), T is the absolute temperature, k_{B} is the

Boltzmann constant, and Q_{PRC}, Q_{PAH} and Q_{OH} are the partition functions of the PRC, the PAH and the OH radical, respectively.

The reaction constant for the formation of the product according to the transition state (TST) theory is expressed as

$$k_2 = \frac{k_B T}{h} \frac{Q^{\ddagger}}{Q_{PRC}} e^{-(E_2 - E_1)/k_B T}, \quad (13)$$

where h is the Planck constant, E_2 is the energy of the transition state with respect to the reference state and $Q^{\ddagger}$ is the partition function of the transition state. According to Equation (11), the product of Equations (12) and (13) gives the total rate constant k

$$k = \frac{k_B T}{h} \frac{Q^{\ddagger}}{Q_{PAH} Q_{OH}} e^{-E_2/k_B T}, \quad (14)$$

an expression in which E_1 no longer appears.

Because we are interested here in the modification of the rate constant k upon physisorption of the PAH on a carbonaceous particle modelling a soot surface, we rather choose to evaluate the ratio of the total rate constant of the oxidation in the gas phase to the one associated with the oxidation in the adsorbed phase, as

$$\frac{k^{ads}}{k^{gas}} = \frac{Q_{PAH}^{gas}}{Q_{PAH}^{ads}} \frac{Q_{OH}^{gas}}{Q_{OH}^{ads}} \frac{Q^{\ddagger,ads}}{Q^{\ddagger,gas}} e^{\frac{-(E_2^{ads} - E_2^{gas})}{k_B T}}. \quad (15)$$

3. Results and discussion

As a first application, we investigate here the details of the heterogeneous oxidation reaction of benzene adsorbed on a soot particle modelled by a large cluster of 80 carbon atoms arranged in fused benzene rings as in a graphene sheet. Note that, as in our previous studies [43–45], the dangling bonds of this cluster have been saturated with hydrogen atoms, and the cluster will thus be referred below as the $C_{80}H_{22}$ cluster. For these adsorbed species, the calculations have been performed with the AM1-D method.

3.1 Determination of the α and R_0 parameters for O–C interactions

First, we have determined the values of the α^{OH} and R_0^{OH} parameters of the damping function used for the calculations of the dispersion contributions to the AM1-D method (see Equation (3)) in the following way. We performed AM1 calculations to characterise the PRC and the TS corresponding to the oxidation reactions of benzene by OH in the gas phase. The results, given in Table 2, show that the equilibrium distance for the PRC is larger than 3.0 Å, and that the equilibrium distance for the corresponding TS is equal to 2.08 Å. To set up our SE-D model, we can thus reasonably think that the dispersion interactions between the incoming OH and the reacting benzene molecule play a significant role above 3.0 Å only, and should vanish between 2.1 and 3.0 Å. This leads us to choose an R_0 value equal to 2.75 Å for the O–C interactions in the OH–benzene system. The corresponding value of the α parameter has been chosen accordingly to ensure a smooth removal of the dispersion interactions between 2.0 and 3.0 Å [38]. Note that the R_0 values defined here are in agreement with the values previously fitted in the literature on the basis of DFT calculations [52]. Note also that we will assume in the following that the parameters selected here for the O–C dispersion interactions are transferable to the calculations of the interactions between OH and soot.

Table 2. Comparison of the energy values and O—C distances obtained using the AM1 and AM1-D methods.

	PRC		TS	
	Energy	d_{C-O}	Energy	d_{C-O}
AM1 gas phase[a]	−4.27	3.17	4.06	2.08
AM1D gas phase	−12.1	2.81	1.26	2.09
AM1D adsorbed phase	−13.9	2.81	−0.98	2.10

Note: The energies are in kJ/mol while the distances in Å.[a] AM1 calculations lead to a gas phase TS energy slightly greater than zero, i.e. TS lies above the reactants. The same is obtained when dispersion is included but with a much smaller magnitude. This result is proper to AM1 methodology applied to benzene molecule. Similar calculations on larger PAHs in the same conditions lead to small negative gas phase TS energies, i.e. TS energy level is always below the energy of the reactants [38]. DFT and *ab initio* calculations on benzene and naphthalene show that the TS is also below the reactants, irrespective of the situation (gas-phase, with or without dispersion) [38,51,53]. This slight discrepancy between AM1 and more sophisticated methods in the case of benzene does not matter since benzene is considered here as a test molecule for our statistical approach explained further.

3.2 Analysis of the OH + PAH energy profile

Here, we present the optimised geometries and adsorption energies of the PRC and TS corresponding to the oxidation of benzene by OH when the benzene molecule is adsorbed on the surface of a $C_{80}H_{22}$ cluster. Note that, we have considered only the situation in which the OH radical comes from the gas phase even for the reaction taking place in the adsorbed phase (i.e. the OH radical arrives perpendicularly to the cluster surface). Indeed, preliminary calculations have shown that the OH radical is captured by the cluster when arriving parallel to its surface, such that the oxidation reaction cannot take place [38]. Moreover, the results obtained for the absorbed species have also been compared with the results of the same kind of calculations performed on gas phase systems with both AM1 and AM1-D methods.

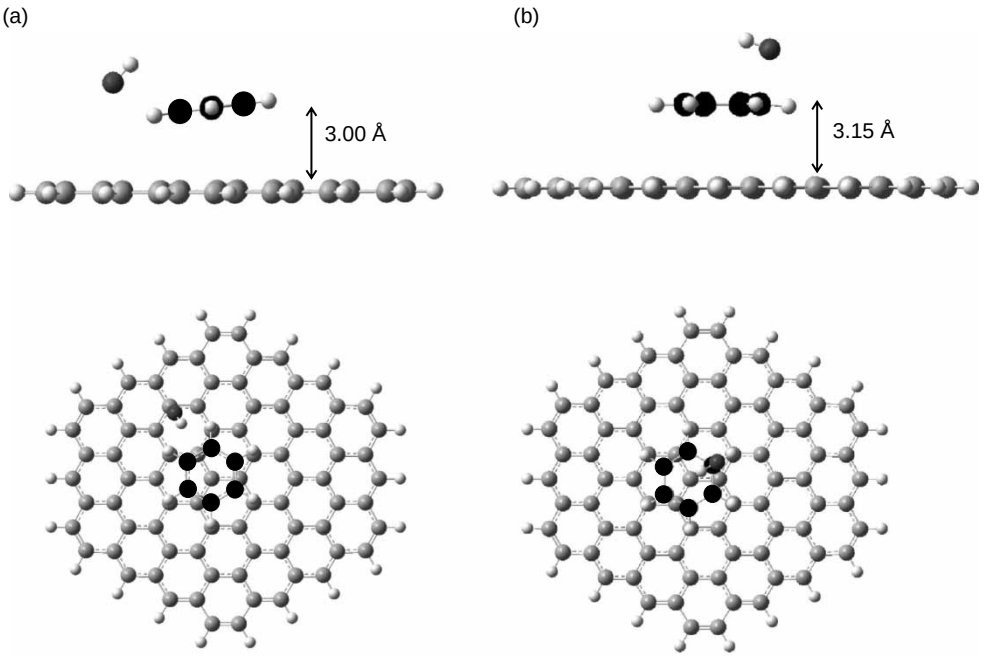

Figure 2. Side (top of the figure) and top (bottom of the figure) views of the geometry of (a) the PRC and (b) the TS obtained for the oxidation reaction by OH of an adsorbed benzene molecule, using AM1-D method. The C atoms of the benzene molecule are represented as black circles for clarity, whereas the C atoms of the graphite cluster are represented as grey circles. Dark grey and white circles represent the O and H atoms, respectively. Note that the nearest C—C distances between the benzene molecule and the surface is also indicated on the side views.

As an illustration of the obtained results, the optimised geometries of the PRC and TS are given in Figure 2 for the benzene + OH system adsorbed on the $C_{80}H_{22}$ cluster. This figure shows that the OH radical approaches the benzene molecule along a direction perpendicular to a C—C bond, in a symmetric position with respect to the two C atoms. This PRC geometry is also found when performing the optimisation for the gas phase system using both AM1-D and AM1 (i.e. without the dispersion contribution) methods. Upon further approach, OH slightly rotates and deviates from its symmetric position, such as the optimised TS geometry corresponds to the attachment of OH directly on one C atom of the benzene molecule. Similar features are calculated both for the gas phase and for the adsorbed phase systems, using both AM1 and AM1-D methods. Note that these geometries are very similar to those obtained from DFT calculations characterising the oxidation reaction in the gas phase [52].

The energy values corresponding to these optimised geometries are given in Table 2 together with the O—C (nearest C atom) distances. First, the values given in Table 2 show that the energy values obtained with the method AM1-D are algebraically lower than the corresponding AM1 values without any dispersion contribution. This result is not surprising since dispersion is an attractive interaction. Also, for the same reason, the O—C distances are shorter when using the AM1-D method, but only for the PRC, showing the greater influence of the dispersion interactions on the PRC than on the TS geometries due to the damping function. Furthermore, the energy values obtained for the adsorbed systems (with the AM1-D method) are algebraically lower than the energy values calculated for the corresponding systems in gas phase with the same method, as a consequence of the attractive interaction between the adsorbed system and the soot surface which thus tends to stabilise the different steps of the oxidation reaction.

3.3 Kinetics of the oxidation reaction: ratio of the rate constants

Before calculating the different partition functions in Equation (15), we have characterised separately the various motions of the benzene molecule and of the TS complex in the gas phase and on the soot surface.

As an illustration of the corresponding results, we give in Figure 3 the energy curves obtained upon rotating the adsorbed benzene molecule around the z-axis, perpendicular to the surface of the $C_{80}H_{22}$ cluster (Figure 3(a)) and around the x-axis parallel to this surface (Figure 3(b)). The energy barriers for the rotational motion around the z-axis (Figure 3(a)) are three times smaller than the k_BT value at room temperature, and, as a consequence this rotational motion can be considered as a free rotation in our

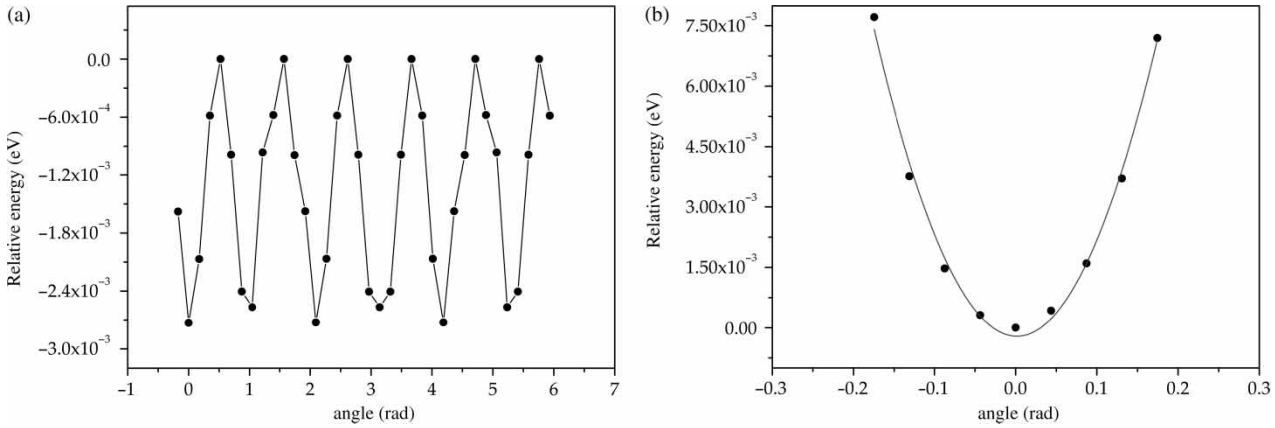

Figure 3. Energy curves obtained upon rotating an adsorbed benzene molecule (a) around the z-axis perpendicular to the surface of the $C_{80}H_{22}$ cluster and (b) around the x axis parallel to this surface. Note that the relative energy (in eV) is defined with respect to the maximum or the minimum of the energy curve. The angles are given in radian.

calculations. In a similar way, Figure 3(b) shows that the energy variations upon slightly tilting the admolecule around the x-axis can be easily represented by considering the admolecule as a 1D harmonic oscillator. In fact, this detailed study shows that all the various motions of the adsorbed benzene molecule and TS can be described, in a first approach, either by free motions as in gas phase or by the rigid rotor and harmonic oscillator approximations. This leads to the following assumptions:

- the translational partition functions in the directions which are parallel to the $C_{80}H_{22}$ cluster surface (direction x and y) are the same in the adsorbed phase and in the gas phase, due to the very weak interaction potential corrugation of the cluster surface,
- for the same reason, the rotation around the z-direction in the adsorbed phase can be approximated by a free rotor.
- by contrast, the translation in the z-direction (i.e. perpendicular to the surface) as well as the rotations around the x and y axes are hindered due to the presence of the cluster surface and have to be treated as vibrational motions.

Moreover, on the basis of the energy calculations presented above, we can use the following additional approximations to calculate the ratio $k^{\text{ads}}/k^{\text{gas}}$:

- the OH radical can be considered as in gas phase, even if the reaction takes place in the adsorbed phase. This assumption is justified by the fact that an OH radical approaching the graphene sheet could be captured such that the oxidation reaction cannot occur [38]. Moreover, the OH radical approaches toward the PAH only from the gas phase above the PAH plane.
- the internal vibrational modes and the electronic states are the same in the adsorbed phase and in the gas phase for the benzene molecule and for the TS, because of the weak interaction with the soot surface characterising a physisorption process.

Using these assumptions, it turns out that the partition function ratios become

$$\frac{Q^{\text{gas}}_{\text{PAH}}}{Q^{\text{ads}}_{\text{PAH}}} = \frac{Q^{\text{gas,PAH}}_{\text{trans},z}}{Q^{\text{ads,PAH}}_{\text{tr}_z\rightarrow\text{vibr}}} \frac{Q^{\text{gas,PAH}}_{\text{rot}}}{Q^{\text{ads,PAH}}_{\text{rot}_x\rightarrow\text{vibr}} Q^{\text{ads,PAH}}_{\text{rot}_y\rightarrow\text{vibr}} Q^{\text{ads,PAH}}_{\text{rot}_z}}, \tag{16}$$

and

$$\frac{Q^{\ddagger,\text{ads}}}{Q^{\ddagger,\text{gas}}} = \frac{Q^{\ddagger,\text{ads}}_{\text{tr}_z\rightarrow\text{vibr}}}{Q^{\ddagger,\text{gas}}_{\text{trans},z}} \frac{Q^{\ddagger,\text{ads}}_{\text{rot}_x\rightarrow\text{vibr}} Q^{\ddagger,\text{ads}}_{\text{rot}_y\rightarrow\text{vibr}} Q^{\ddagger,\text{ads}}_{\text{rot}_z}}{Q^{\ddagger,\text{gas}}_{\text{rot}}}. \tag{17}$$

Finally, replacing the above equations into Equation (15), we arrive at the following expression of the rate constants ratio,

$$\frac{k^{\text{ads}}}{k^{\text{gas}}} = \frac{Q^{\text{gas,PAH}}_{\text{trans},z}}{Q^{\text{ads,PAH}}_{\text{tr}_z\rightarrow\text{vibr}}} \frac{Q^{\text{gas,PAH}}_{\text{rot}}}{Q^{\text{ads,PAH}}_{\text{rot}_x\rightarrow\text{vibr}} Q^{\text{ads,PAH}}_{\text{rot}_y\rightarrow\text{vibr}} Q^{\text{ads,PAH}}_{\text{rot}_z}} \times \frac{Q^{\ddagger,\text{ads}}_{\text{tr}_z\rightarrow\text{vibr}}}{Q^{\ddagger,\text{gas}}_{\text{trans},z}} \frac{Q^{\ddagger,\text{ads}}_{\text{rot}_x\rightarrow\text{vibr}} Q^{\ddagger,\text{ads}}_{\text{rot}_y\rightarrow\text{vibr}} Q^{\ddagger,\text{ads}}_{\text{rot}_z}}{Q^{\ddagger,\text{gas}}_{\text{rot}}} \text{e}^{\frac{-\left(E_2^{\text{ads}} - E_2^{\text{gas}}\right)}{k_{\text{B}}T}}. \tag{18}$$

where the following analytical expressions, valid for 1D and 3D rotations, 1D translation and 1D harmonic vibration, respectively, can be used for the calculations of the partition functions:

$$Q^{\text{1D}}_{\text{trans}} = L\sqrt{\frac{mk_{\text{B}}T}{2\pi\hbar^2}}, \tag{19}$$

Table 3. Molecular constants corresponding to the different type of motions.

		PAH (benzene)	TS (benzene + OH)
Gas phase	Translation	$M = 1.29 \times 10^{-25}$ kg	$M = 1.58 \times 10^{-25}$ kg
	Rotation	$I_1 = 29.5 \times 10^{-46}$ kg m^2	$I_1 = 41.2 \times 10^{-46}$ kg m^2
		$I_2 = 14.8 \times 10^{-46}$ kg m^2	$I_2 = 32.1 \times 10^{-46}$ kg m^2
		$I_3 = 14.8 \times 10^{-46}$ kg m^2	$I_3 = 20.8 \times 10^{-46}$ kg m^2
		$\sigma = 12$	$\sigma = 1$
Adsorbed phase	Trans → vibr	$M = 1.29 \times 10^{-25}$ kg	$M = 1.58 \times 10^{-25}$ kg
		$\nu = 1.57 \times 10^{12}$ s^{-1}	$\nu = 1.42 \times 10^{12}$ s^{-1}
	Rot$_x$ → vibr	$I_x = 14.8 \times 10^{-46}$ kg m^2	$I_x = 53.4 \times 10^{-46}$ kg m^2
		$\nu = 1.16 \times 10^{12}$ s^{-1}	$\nu = 1.44 \times 10^{12}$ s^{-1}
	Rot$_y$ → vibr	$I_y = 14.8 \times 10^{-46}$ kg m^2	$I_y = 26.6 \times 10^{-46}$ kg m^2
		$\nu = 1.17 \times 10^{12}$ s^{-1}	$\nu = 9.12 \times 10^{11}$ s^{-1}
	Rotation$_z$	$I_z = 29.5 \times 10^{-46}$ kg m^2	$I_z = 37.5 \times 10^{-46}$ kg m^2
		$\sigma = 6$	$\sigma = 1$

$$Q_{\text{vibr}} = \frac{1}{1 - e^{\frac{-h\nu}{k_B T}}}, \tag{20}$$

$$Q_{\text{rot}}^{\text{1D}} = \frac{1}{\sigma}\sqrt{\frac{8\pi k_B T}{\hbar^2} I}, \tag{21}$$

$$Q_{\text{rot}}^{\text{3D}} = \frac{8\pi^2}{\sigma}\left(\frac{k_B T}{2\pi\hbar^2}\right)^{3/2}\sqrt{I_1 I_2 I_3}. \tag{22}$$

In the above equations, $\hbar$ is the Planck constant divided by 2π, ν is the vibrational frequency and σ is the symmetry number of the rotation. L is the finite distance (of arbitrary large extension) along which the molecule of mass m is permitted to move. I is a 1D moment of inertia associated with the rotation axis defined in Equation (21) and I_1, I_2 and I_3 are the three moments of inertia of a 3D rotor.

To obtain the vibrational frequencies of the various hindered rotational motions we tilted the given molecule around its equilibrium position. The rotations are performed by small angles around the x and y axis parallel to the soot surface and we calculated the energy in the tilted positions (but we did not optimise it). Then, the obtained energy values were fitted by a quadratic function:

$$E_{\text{pot}} = \frac{1}{2}k(x - x_0)^2 + a, \tag{23}$$

in which x denotes the tilt angle. The force constant k was then used for determining the frequency:

$$\nu = \frac{1}{2\pi}\sqrt{\frac{k}{I}}, \tag{24}$$

where I is the corresponding moment of inertia.

A similar procedure was repeated for the vibrational motion (i.e. hindered translational motion) along the z-axis, but by replacing the moment of inertia by the mass of the admolecule in Equation (24).

The moment of inertia in the adsorbed phase was calculated around an axis perpendicular to the surface and passing through the centre of mass of the admolecule. Note that, this axis was considered as the z-axis in our calculations.

The various constants corresponding to the different type of motions are collected in Table 3, and the partition functions calculated for the benzene molecule and the corresponding TS complex are given in Table 4. By using these values in Equation (18), we calculate that $k^{\text{ads}}/k^{\text{gas}} = 0.69$, indicating that the oxidation reaction of a benzene molecule by OH is slightly hindered when the molecule is adsorbed on a graphene sheet.

This result is not too surprising because the adsorption of the PAH on the graphene sheet prevents from the OH attack from one side of the PAH plane. Then, we expect

Table 4. Molecular partition functions of the different type of motions.

		PAH (benzene)	TS (benzene + OH)
Gas phase	Translation	$8.73 \times 10^{10} \times L$ m^{-1}	$9.63 \times 10^{10} \times L$ m^{-1}
	Rotation	7.53×10^3	1.87×10^5
Adsorbed phase	Trans → vibr	4.48	4.89
	Rot$_x$ → vibr	5.85	4.84
	Rot$_y$ → vibr	5.81	7.32
	Rotation$_z$	27.6	187

from this simple argument that the rate constant should be more or less divided by a factor of two with respect to the reaction in gas phase. Although this is a reductive reasoning, it gives some confidence on the application of our SE-D model to reactivity problems. Note that our model has been built to allow also the simulation of gas-surface processes on which the surface can carry some defects like Stone–Wales defects [57], in the plane and edge atom vacancies [58]. Of course, the modification of the reactivity on a defective surface is expected to be very different and non predictable *a priori* with respect to the perfect surface analysed here. But, in this latter case, the conclusion is in accordance with the results of our energy optimisation process, (see above) which shows that the soot particle stabilises the OH + benzene PRC and the corresponding TS with respect to the gas phase situation.

4. Conclusions

In the present paper, we have used the AM1-D method to characterise the oxidation by the OH of a PAH molecule adsorbed on a soot surface modelled by a graphene-like cluster. This method is based on an electrostatic and induction contribution calculated at the SCF AM1 level associated with a sum of two-body dispersion terms of the $C^{(6)}/R^6$ form [37]. Indeed, the AM1-D is able to properly describe the interactions between large aromatic systems, and it can be used to study systems for which full *ab initio* calculations are prohibited because of their large size. As a first application, we have detailed the oxidation mechanism for benzene, which is the simplest aromatic molecule (although not strictly a PAH molecule!). We have thus compared the characteristics of the oxidation reaction for the adsorbed benzene with that of the corresponding reaction in the gas phase. The main conclusion of the present work is a clear inhibition of the oxidation process by the adsorption of the benzene molecule on the soot surface modelled here. This conclusion is in qualitative agreement with previous experimental observations, concerning, however, larger PAH molecules on graphene surfaces [21]. For a better comparison with these experimental results, further investigations devoted to naphthalene, phenanthrene and anthracene molecules are under consideration. However, the corresponding calculations are much more complex due to the presence of different non-equivalent carbon sites for the OH attachment in the oxidation mechanism. Moreover, the real surface of soot is certainly not free of defects, and it would be thus also important to characterise the oxidation reactions of PAH molecules adsorbed on defective carbonaceous surfaces.

Acknowledgements

G.H.'s PhD is partly granted by the French Government which is gratefully acknowledged.

References

[1] B.J. Finlayson-Pitts and J.N. Pitt Jr, *Chemistry of the Upper and Lower Atmosphere: Theory, Experiments, and Applications*, Academic Press, San Diego, 2000.
[2] R.C. Pierce and M. Katz, *Dependency of polynuclear aromatic hydrocarbon content on size distribution of atmospheric aerosols*, Environ. Sci. Technol. 9 (1975), pp. 347–353.
[3] U. Pöschl, T. Letzel, C. Schauer, and R. Niessner, *Interaction of ozone and water vapor with spark discharge soot aerosol particles coated with benzo[a]pyrene: O_3 and H_2O adsorption, benzo[a]pyrene degradation, and atmospheric implications*, J. Phys. Chem. A 105 (2001), pp. 4029–4041.
[4] D.G. Aubin and J.P.D. Abbatt, *Laboratory measurements of thermodynamics of adsorption of small aromatic gases to* n*-hexane soot surfaces*, Environ. Sci. Technol. 40 (2006), pp. 179–187.
[5] N.O.A. Kwamena, J.A. Thornton, and J.P.D. Abbatt, *Kinetics of surface-bound benzo[a]pyrene and ozone on solid organic and salt aerosols*, J. Phys. Chem. A 108 (2004), pp. 11626–11634.
[6] N.O.A. Kwamena, M.E. Earp, C.J. Young, and J.P.D. Abbatt, *Kinetic and product yield study of the heterogeneous gas–surface reaction of anthracene and ozone*, J. Phys. Chem. A 110 (2006), pp. 3638–3646.
[7] N.O.A. Kwamena, M.G. Staikova, D.J. Donaldson, I.J. George, and J.P.D. Abbatt, *Role of the aerosol substrate in the heterogeneous ozonation reactions at the surface-bound PAHs*, J. Phys. Chem. A 111 (2007), pp. 11050–11058.
[8] R. Kotzick, U. Panne, and R. Niessner, *Changes in condensation properties of ultrafine carbon particles subjected to oxidation by ozone*, J. Aerosol. Sci. 28 (1997), pp. 725–735.
[9] T. Novakov and C.E. Corrigan, *Cloud condensation nucleus activity of the organic component of biomass smoke particles*, Geophys. Res. Lett. 23 (1996), pp. 2141–2144.
[10] C.N. Cruz and S.N. Pandis, *A study of the ability of pure secondary organic aerosol to act as cloud condensation nuclei*, Atmos. Environ. 31 (1997), pp. 2205–2214.
[11] J.H. Seinfeld and S.N. Pandis, *Atmospheric Chemistry and Physics*, John Wiley and Sons, New York, 1998.
[12] G.T. Wolf and R.L. Klimisch (eds.), *Particulate Carbon, Atmospheric Life Cycle*, Plenum Press, New York, 1982.
[13] E.D. Goldberg, *Black Carbon in the Environment: Properties and Distribution*, Wiley, New York, 1985.
[14] J. Dachs and S.J. Eisenreich, *Adsorption onto aerosol soot carbon dominates gas–particle partitioning of polycyclic aromatic hydrocarbons*, Environ. Sci. Technol. 34 (2000), pp. 3690–3697.
[15] M.O. Andreae and A. Gelencser, *Black carbon or brown carbon? The nature of light-absorbing carbonaceous aerosols*, Atmos. Chem. Phys. 6 (2006), pp. 3131–3148.
[16] E.F. Mikhailov and S.S. Vlasenko, *Structure and optical properties of soot aerosols in a moist atmosphere: 2. Influence of hydrophilicity of particles on the extinction, scattering, and absorption coefficients*, Atmos. Ocean. Phys. 43 (2007), pp. 195–207.
[17] J.B. Renard, D. Daugeron, P. Personne, G. Legros, J. Baillargeat, E. Hadamcik, and J.C. Worms, *Optical properties of randomly distributed soot: improved polarimetric and intensity scattering functions*, Appl. Opt. 44 (2005), pp. 591–596.
[18] O.B. Popovicheva and A.M. Starik, *Aircraff-generated soot aerosols: physicochemical properties and effect of emission into the atmosphere*, Atmos. Ocean. Phys. 43 (2007), pp. 147–164.
[19] D. Delhaye, *Experimental characterization of the physico-chemical properties of soot particles emitted by an aircraft engine*, PhD thesis, Marseille, France, 2007.
[20] R.L. Vander Wal and A.J. Tomasek, *Soot nanostructure: dependence upon synthesis conditions*, Combust. Flame 136 (2004), pp. 129–140.
[21] W. Esteve, H. Budzinski, and E. Villenave, *Relative rate constant for the heterogeneous reactions of OH, NO_2 and NO radicals with polycyclic aromatic hydrocarbons adsorbed on carbonaceous particles. Part 1: PAHs adsorbed on 1–2 μm calibrated graphite particles*, Atmos. Environ. 38 (2004), pp. 6063–6072.
[22] E. Perraudin, H. Budzinski, and E. Villenave, *Analysis of polycyclic aromatic hydrocarbons adsorbed on particles of atmospheric*

interest using pressurized fluid extraction, Anal. Bioanal. Chem. 383 (2005), pp. 122–131.
[23] P.J. DeMott, Y. Chen, S.M. Kreidenweis, L.M. McInnes, D.C. Rogers, and D.E. Sherman, *Ice Formation by Black Carbon Particles*, Geophys. Rev. Lett. 26 (1999), pp. 2429–2432.
[24] H. Saathoff, K.-H. Naumann, N. Riemer, S. Kamm, O. Möhler, U. Schurath, H. Vogel, and B. Vogel, *The Loss of NO_2, HNO_3, NO_3/N_2O_5, and $HO_2/HOONO_2$ on soot aerosol: a chamber and modeling study*, Geophys. Rev. Lett. 28 (2001), pp. 1957–1960.
[25] M. Wentzel, H. Gorzamski, K.-H. Naumann, H. Saathoff, and S. Weinbruch, *Transmission electron microscopy and aerosol dynamical characterization of soot aerosols*, J. Aerosol. Sci. 34 (2003), pp. 1347–1370.
[26] A.R. Chughtai, N.J. Miller, D.M. Smith, and J.R. Pitts, *Carbonaceous particle hydration III*, J. Atmos. Chem. 34 (1999), pp. 259–279.
[27] M.S. Munoz Salgado and M. Rossi, *Heterogeneous reactions of HNO_3 with flame soot generator under different combustion conditions. Reaction mechanism and kinetics*, Phys. Chem. Chem. Phys. 4 (2002), pp. 5110–5118.
[28] J.M.E. Storey and J.F. Pankow, *Gas–particle partitioning of semi-volatile organic compounds to model atmospheric particulate materials – I. Sorption to graphite, sodium chloride, alumina, and silica particles under low humidity conditions*, Atmos. Environ. A 26 (1992), pp. 435–443.
[29] K.U. Goss and S.J. Eisenreich, *Sorption of volatile organic compounds to particles from a combustion source at different temperatures and relative humidities*, Atmos. Environ. 31 (1997), pp. 2827–2834.
[30] B.T. Mader and J.F. Pankow, *Study of the effects of particle-phase carbon on the gas/particle partitioning of semivolatile organic compounds in the atmosphere using controlled field experiments*, Environ. Sci. Technol. 36 (2002), pp. 5218–5228.
[31] B. Ngabé and L. Poissant, *Polycyclic aromatic hydrocarbons in the air in the St. Lawrence Basin (Québec)*, Environ. Sci. Technol. 37 (2003), pp. 2094–2099.
[32] N.K. Lee, S. Park, and S.L. Kim, Ab initio *studies on the van der Waals complexes of polycyclic aromatic hydrocarbons. I. Benzene – naphthalene complex*, J. Chem. Phys. 116 (2002), pp. 7902–7909.
[33] M.O. Sinnokrot, E.F. Valeev, and C.D. Sherrill, *Estimates of the* ab initio *limit for $\pi-\pi$ interactions: the benzene dimer*, J. Am. Chem. Soc. 124 (2002), pp. 10887–10893.
[34] C. Gonzales, T.C. Allison, and E.C. Lim, *Hartree–Fock dispersion probe of the equilibrium structures of small microclusters of benzene and naphthalene: comparison with second-order Møeller–Plesset geometries*, J. Phys. Chem. A 105 (2001), pp. 10583–10587.
[35] C. Gonzales and E.C. Lim, *Evaluation of the Hartree–Fock dispersion (HFD) model as a practical tool for probing intermolecular potentials of small aromatic clusters: comparison of the HFD and MP2 intermolecular potentials*, J. Phys. Chem. A 107 (2003), pp. 10105–10110.
[36] J. Hepburn, G. Scoles, and R. Penco, *A simple but reliable method for the prediction of intermolecular potentials*, Chem. Phys. Lett. 36 (1975), pp. 451–456.
[37] B. Collignon, P.N.M. Hoang, S. Picaud, D. Liotard, M.T. Rayez, and J.C. Rayez, *A semi-empirical potential model for calculating interactions between large aromatic molecules and graphite surfaces*, J. Mol. Struct. Theochem. 772 (2006), pp. 1–12.
[38] B. Collignon, *Modelling at a molecular level of aircraft soot particles and of their interactions with surrounding molecules*, PhD thesis, Besançon, France, 2006.
[39] M.I. Bernal-Uruchurtu, M.T.C. Martins-Costa, C. Millot, and M.F. Ruiz-López, *Improving description of hydrogen bonds at the semiempirical level: water–water interactions as test case*, J. Comp. Chem. 21 (2000), pp. 572–581.
[40] M.I. Bernal-Uruchurtu and M.F. Ruiz-López, *Basic ideas for the correction of semiempirical methods describing H-bonded systems*, Chem. Phys. Lett. 330 (2000), pp. 118–124.
[41] W. Harb, M.I. Bernal-Uruchurtu, and M.F. Ruiz-López, *An improved semiempirical method for hydrated systems*, Theor. Chem. Acc. 112 (2004), pp. 204–216.
[42] J.P. McNamara and I.H. Hillier, *Semi-empirical molecular orbital methods including dispersion corrections for the accurate predictions of the full range of intermolecular interactions in biomolecules*, Phys. Chem. Chem. Phys. 9 (2007), pp. 2362–2370.
[43] S. Hamad, J.A. Mejias, S. Lago, S. Picaud, and P.N.M. Hoang, *A theoretical study of the adsorption of water on a model soot surface. I. Quantum chemical calculations*, J. Phys. Chem. B 108 (2004), pp. 5405–5409.
[44] B. Collignon, P.N.M. Hoang, S. Picaud, and J.C. Rayez, *Clustering of water molecules on model soot particles: an* ab initio *study*, Comp. Lett. 1 (2005), pp. 277–287.
[45] B. Collignon, P.N.M. Hoang, S. Picaud, and J.C. Rayez, Ab initio *study of the water adsorption on hydroxylated graphite surfaces*, Chem. Phys. Lett. 406 (2005), pp. 430–435.
[46] G.C. Maitland, M. Rigby, E.R. Smith, and W.A. Wakeham, *Intermolecular Forces, their Origin and Determination*, Oxford Science Publications, Oxford, 1987.
[47] S. Picaud, P.N.M. Hoang, S. Hamad, J.A. Mejias, and S. Lago, *A theoretical study of the adsorption of water on a model soot surface. II. Molecular dynamics simulations*, J. Phys. Chem. B 108 (2004), pp. 5410–5415.
[48] T. Werder, J.H. Walther, R.L. Jaffe, T. Halicioglu, and P. Koumoutsakos, *On the water–carbon interaction for use in molecular dynamics simulations of graphite and carbon nanotubes*, J. Phys. Chem. B 107 (2003), pp. 1345–1352.
[49] A. Alexiadis and S. Kassinos, *Molecular simulation of water in carbon nanotube*, Chem. Rev. 108 (2008), pp. 5014–5034.
[50] I.W.M. Smith and A.R. Ravishankara, *Role of hydrogen-bonded intermediates in the bimolecular reactions of the hydroxyl radical*, J. Phys. Chem. A 106 (2002), pp. 4798–4807.
[51] I.V. Tokmakov and M.C. Lin, *Kinetics and mechanism of the $OH + C_6H_6$ reaction: a detailed analysis with first-principles calculations*, J. Phys. Chem. A 106 (2002), pp. 11309–11326.
[52] S. Raoult, *Theoretical contribution to the understanding of oxidation mechanisms of some aromatic compounds in the troposphere (benzene, toluene, phenol)*, PhD thesis, Université Bordeaux 1, France, 2003.
[53] S. Raoult, M.T. Rayez, J.C. Rayez, and R. Lesclaux, *Gas phase oxidation of benzene: kinetics, thermochemistry and mechanism of initial steps*, Phys. Chem. Chem. Phys. 6 (2004), pp. 2245–2253.
[54] V.H. Uc, I. Garcia-Cruz, A. Hernandez-Laguna, and A. Vivier-Bunge, *New channels in the reaction mechanism of the atmospheric oxidation of toluene*, J. Phys. Chem. A 104 (2000), pp. 7847–7855.
[55] M.J. Lundqvist and L.A. Eriksson, *Hydroxyl radical reactions with phenol as a model for generation of biologically reactive tyrosyl radicals*, J. Phys. Chem. B 104 (2000), pp. 848–855.
[56] R. Atkinson and R.J. Cvetanovic, *Activation energies of the addition of $O(^3P)$ atoms to olefins*, J. Chem. Phys. 56 (1972), pp. 432–437.
[57] A.J. Stone and D.J. Wales, *Theoretical studies of icosahedral C_{60} and some related species*, Chem. Phys. Lett. 128 (1986), pp. 501–503.
[58] G. Ghigo, A. Maranzana, G. Tonachini, C.M. Zicovich-Wilson, and M. Causa, *Modeling soot and its functionalization under atmospheric or combustion conditions by density functional theory within molecular (polycyclic-aromatic-hydrocarbon-like) and periodic methodologies*, J. Phys. Chem. B 108 (2004), pp. 3215–3223.